2010

The applicability of three-dimensional aromaticity in BiSnn- Zintl analogues

Penee A. Clayborne
Virginia Commonwealth University, University of Jyvaskyla

Ujjwal Gupta
The Pennsylvania State University

Arthur C. Reber
Virginia Commonwealth University

See next page for additional authors

The applicability of three-dimensional aromaticity in $BiSn_n^-$ Zintl analogues

Peneé A. Clayborne,[1,2] Ujjwal Gupta,[3] Arthur C. Reber,[1] Joshua J. Melko,[3] Shiv N. Khanna,[1,a)] and A. W. Castleman, Jr.[3,b)]
[1]*Department of Physics, Virginia Commonwealth University, Richmond, Virginia 23284, USA*
[2]*Department of Chemistry, Nanoscience Center, University of Jyväskylä, Jyväskylä FI-40014, Finland*
[3]*Department of Chemistry and Department of Physics, The Pennsylvania State University, University Park, Pennsylvania 16802, USA*

(Received 7 July 2010; accepted 18 August 2010; published online 1 October 2010)

Three-dimensional aromaticity is shown to play a role in the stability of deltahedral Zintl clusters and here we examine the connection between aromaticity and stability. In order to gain further insight, we have studied Zintl analogs comprised of bismuth doped tin clusters with photoelectron spectroscopy and theoretical methods. To assign aromaticity, we examine the ring currents induced around the cage by using the nucleus independent chemical shift. In the current study, $BiSn_4^-$ is a stable cluster and fits aromatic criteria, while $BiSn_5^-$ is found to fit antiaromatic criteria and has reduced stability. The more stable clusters exhibit an aromatic character which originates from weakly interacting *s*-states and bonding orbitals parallel to the surface of the cluster, while nonbonding lone pairs perpendicular to the surface of the cluster account for antiaromaticity and reduced stability. The effect of three-dimensional aromaticity on the electronic structure does not result in degeneracies, so the resulting variations in stability are smaller than those seen in conventional aromaticity. © *2010 American Institute of Physics*. [doi:10.1063/1.3488103]

I. INTRODUCTION

Zintl ions are the multiply charged polyatomic anions of post-transition metals and semimetal atoms[1–5] that can combine with electropositive elements such as alkali atoms to form Zintl phases, representing an important class of cluster assembled materials. The bonding within individual Zintl ions is covalent while the solid is stabilized by the ionic interactions between the multiply charged anions and the countercations. The resulting properties are consequently governed by the electronic spectrum of the Zintl ions modulated by the architecture of the resulting solid. Studying the stability of Zintl ions and identifying new stable motifs with different composition and charge state is then an important step toward developing other Zintl-like cluster assembled materials with tunable characteristics.[6–17] One approach toward such an objective is to study isolated Zintl cluster analogs in the gas phase[18–30] through a synergistic effort, combining experiments employing mass spectrometry and photoelectron spectroscopy with corresponding theoretical studies to provide information on the stability and electronic character. We have previously reported such an effort and shown how the substitution of tin atoms by bismuth in nine atom deltahedral gas phase Zintl anions suppresses the fluxionality of these clusters and increases the size of the cage for endohedral doping.[19] Here, we study the $BiSn_n^-$ gas phase Zintl analogs of Sn_n^{2-} in an effort to understand what controls the stability of these cage clusters, which may lead to new cluster building blocks with varying charge states.

The stability of Zintl ions is often reconciled within Wade–Mingos rules,[31,32] where the clusters with $2n+2$ skeletal electrons form the most spherical deltahedra, where n is the number of vertex atoms. As Bi has one more electron than Sn, such a rule would predict that all $BiSn_n^-$ clusters should be stable as deltahedral clusters. Although these clusters do follow Wade–Mingo's rules, they have differing relative stability that in some cases may involve three-dimensional aromaticity,[33–36] which has been proposed as a tool for identifying stable cage compounds. Three-dimensional aromaticity differs from its better known counterpart two-dimensional aromaticity.[37] In two-dimensional aromaticity, the π or σ electrons in planar systems may be thought of as a free electron gas confined to a ring. Systems that contain $4n+2$ electrons (where n is an integer) and have a large highest occupied molecular orbital-lowest unoccupied molecular orbital (HOMO-LUMO) gap are considered stable and aromatic, according to Hückel's rule.[38] However, clusters with $4n$ electrons are marked by an unfilled degenerate highest occupied molecular orbital, which can result in either a Jahn–Teller distortion or a triplet spin state, and both consequences result in reduced stability. Previously observed all-metal two-dimensional aromatic clusters include Al_4^{2-}, Al_3X (X=Sb, As), and Al_3Bi in the gas phase[39–41] and $[Te_2As_2]^{2-}$, which has been synthesized[42] in the solid state. In three-dimensional aromaticity, one considers the valence electrons of the cluster or π electrons in the fullerene to be a free electron gas confined to the surface of a sphere. The resulting electronic structure has a gap for $2(N+1)^2$ electrons (where N is an integer), which corresponds to the spherical harmonics, known as Hirsch's rule.[43] In the clusters studied here, however, the clusters are not particularly metallic, so such simple electron counting rules are ineffectual. Instead, a more useful criteria for determining the aromatic character of

a)Author to whom correspondence should be addressed. Electronic mail: snkhanna@vcu.edu.
b)Electronic mail: awc@psu.edu.

both two-dimensional and three-dimensional clusters is by examining the delocalization of electrons and the resulting diatropic (negative) nucleus independent chemical shift (NICS) value.[44,45]

Antiaromatic clusters are identified by their paratropic (positive) NICS values because the magnetic field induces a ring current which strongly affects the local magnetic environment. The direction of the induced magnetic field depends on the orientation of the orbitals; the fewer the nodes in the molecular orbitals around the ring or cage, the more diatropic the NICS value, while antibonding or nonbonding *p*-orbitals along the ring or perpendicular to the cage are most likely to produce a paratropic shift. Examples of antiaromatic all-metal clusters have been shown to exist theoretically but there have been very few seen experimentally. The gas phase cluster $Li_3Al_4^-$ was believed to be antiaromatic[46] but later Chen *et al.*,[47] using molecular orbital NICS (MO-NICS), found the cluster to be of mixed aromaticity and net aromatic. Other studies have attempted to harness the antiaromatic character in gas phase experiments by adding counterions such as Na or K, but the results have not produced a gas phase antiaromatic cluster, such as the nonaromatic ($K^+[Sn_{12}]^{2-}$) (Refs. 48 and 49) and $NaSi_6^-$, which in the ground state is shown to be aromatic.[50] Many authors have predicted that the E_6^{2-} clusters (E=Si,Ge,Sn,Pb) are antiaromatic,[34,51] but only the Zintl ion Sn_6^{2-} has been synthesized in the solid phase.[52]

In this paper, we report a gas phase study of the tin Zintl dianions known in solution by substituting one tin atom with bismuth, creating singly charged $Bi_xSn_y^-$ clusters. We compare the abundance, stability, aromaticity, and other properties of the clusters. $BiSn_4^-$ and $BiSn_8^-$ reveal increased stability, while reduced stability is found in $BiSn_5^-$ and $BiSn_6^-$. Further, we show how the concepts of aromaticity and antiaromaticity may be applied to understand the stability of Zintl analog clusters.

II. EXPERIMENTAL METHOD

The details of the apparatus employed in this study have been described elsewhere.[53] In brief, $Bi_xSn_y^-$ clusters were formed by using a 1/4 in. 50:50 molar ratio Sn–Bi molded rod in a laser vaporization source. Helium was used as a carrier gas and the clusters were mass analyzed using Wiley McLaren time-of-flight mass spectrometry.[54] The photoelectron spectra for the clusters were obtained using a magnetic bottle time-of-flight photoelectron spectrometer,[55] employing photons from a 308 nm excimer laser, and using velocity map imaging,[27] employing photons from a 355 nm third harmonic Nd:YAG laser for electron detachment. A beam of mass selected anions is crossed with a photon beam to analyze the kinetic energies of the photodetached electrons. If $h\nu$ is the energy of the photon and e^-KE is the measured kinetic energy of the emitted electron, the difference ($h\nu - e^-KE$) provides a direct measure of the energy required to make a transition from the anion of multiplicity M to neutral clusters with multiplicity $M \pm 1$. As the transition to the neutral cluster can occur to the ground or excited states of the multiplicity $M \pm 1$, the photodetachment spectrum

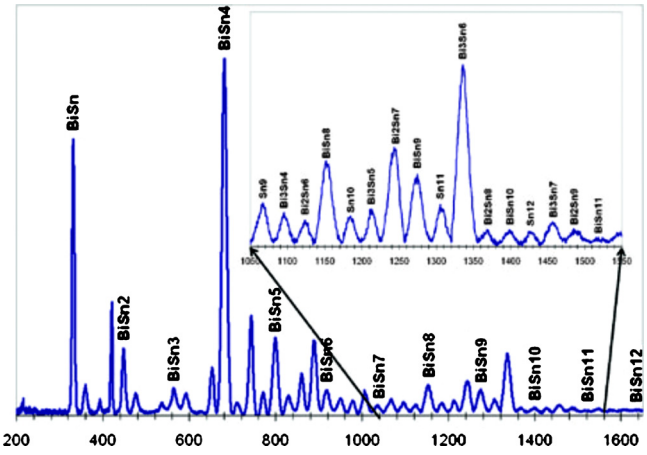

FIG. 1. Collected mass spectrum of $BiSn_n^-$ clusters. The inset is a magnified portion of the $Bi_xSn_y^-$ cluster production.

provides a fingerprint of the electronic structure for comparison with the theoretical calculations. When the calculated transitions agree with the experiment, it can reasonably be assumed that the calculated ground state, including its multiplicity, should be correct. For velocity map images (VMI), three-dimensional distributions are reconstructed from raw images using the BASEX software[56] before obtaining velocity distributions and corresponding photoelectron spectra.

III. THEORETICAL METHOD

First-principles electronic structure studies on the anion and neutral forms of $BiSn_n$ (n=2–11) clusters were performed within a gradient corrected density functional formalism. The calculations were carried out using the ADF (Ref. 57) set of codes while using the BP86 generalized gradient approximation[58,59] for exchange and correlation. We note that we find essentially identical results with the PBE functional[60] and find good agreement between the photoelectron spectra and theoretical results. For Bi and Sn, we employed a quadruple-ζ basis with polarization functions basis set with an all electron calculation that incorporates the zeroth order regular approximation for relativistic effects.[61] Higher order vertical detachment energies (VDE) were calculated by adding the appropriate time dependent-density functional theory (TD-DFT) excitation energy to the vertical detachment energy. The NICS and MO-NICS were calculated by finding the NMR shift of a ghost atom at the center of the cage using the supplemental EPR program as implemented in the ADF code.[62]

IV. RESULTS

A typical mass spectrum of $Bi_xSn_y^-$ clusters is shown in Fig. 1. In this work we concentrate on the singly doped tin clusters $BiSn_{(1-11)}^-$. It is observed from the $BiSn_n^-$ series that $BiSn_4^-$ is especially abundant and that $BiSn_8^-$ and $BiSn_9^-$ are more abundant, which is an indication of enhanced stability, than $BiSn_6^-$, $BiSn_7^-$, $BiSn_{10}^-$, and $BiSn_{11}^-$. The magnetic bottle spectra of $BiSn_{(1-9)}^-$ are shown in Fig. 2, along with VMI images of $BiSn_{(1-6)}^-$. Table I presents the adiabatic electron detachment energies and vertical detachment ener-

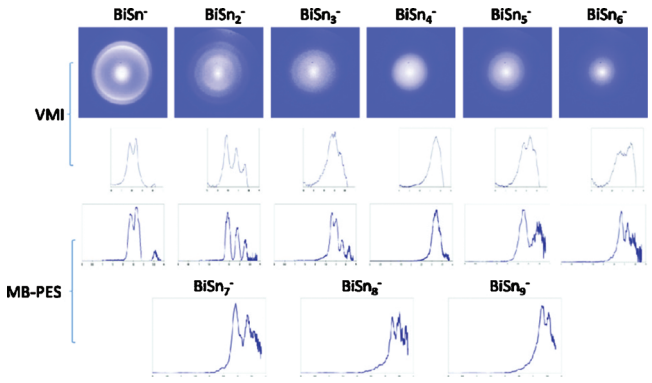

FIG. 2. Velocity map images and corresponding spectra of $BiSn_n^-$ clusters (n=1–6) are given in panel a. Magnetic bottle photoelectron spectra are given in panel b for $BiSn_n^-$ clusters (n=1–9).

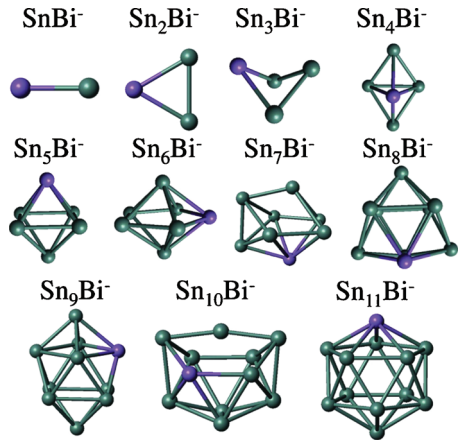

FIG. 3. Lowest energy structures for the $BiSn_n^-$ clusters (n=1–11). The gray and pink spheres represent the tin and bismuth atoms, respectively.

gies for the clusters. The beta parameters for $BiSn_{(1-6)}^-$ are provided in the supporting information.[63] While $BiSn_{10}^-$ and $BiSn_{11}^-$ can be observed in the mass spectrum, the intensity of the clusters was not sufficient to collect photoelectron spectra. It can be seen that $BiSn_4^-$, $BiSn_8^-$, and $BiSn_9^-$ have higher adiabatic detachment energies (ADEs), another pointer of enhanced stability.

The main effect of the bismuth dopant is to change the valence electron count of the cluster. The tin atom has two *s* electrons and two *p* electrons in its valence shell ($5s^25p^2$), which is one less valence electron than the bismuth atom ($6s^26p^3$). One can view the bismuth atom as a negatively charged tin atom (Sn^-); thus, replacing one tin atom with a bismuth atom on pure tin clusters and adding an electron, we have gas phase clusters ($BiSn_4^-$, $BiSn_8^-$, and $BiSn_9^-$) that should be isoelectronic with the more famous Zintl ions (Sn_5^{2-}, Sn_9^{2-}, and Sn_{10}^{2-}). Inspection of the molecular orbitals (Fig. S1) (Ref. 63) of the $BiSn_4^-$ cluster shows that they are indeed virtually identical to those found in Sn_5^{2-}. This similarity allows us to classify $BiSn_4^-$ as a gas phase Zintl analog of Sn_5^{2-}. Equivalent arguments can be applied to all $BiSn_n^-$ clusters, making them isoelectronic with Sn_{n+1}^{2-}. Note that isolated multiply charged clusters are difficult to study because they have negative electron affinities when isolated, and while they may be stabilized in the solid state, the stability of the Zintl phases depends partly on the packing of the solid and the character of the counterion. Hence, a direct comparison of the cluster's stability is nontrivial.[18,64]

We have calculated the global minimum structures for the $BiSn_n^-$ clusters and found that they are deltahedral clusters, consistent with Wade–Mingos rules. The structures are given in Fig. 3, where n=1–11. The structures obtained for $BiSn_3^-$, $BiSn_4^-$, and $BiSn_5^-$ are in agreement with those previously reported by Sun *et al.*[65] Notice that in all cases, the structures are closo deltahedral structures, as is expected, with the same geometrical shapes as their Sn_n^{2-} counterparts. $Sn_{11}Bi^-$ has an icosahedral structure which is essentially identical to that of stannaspherene[48] and the doped stannaspherenes.[30] The primary differences are due to the larger size of the Bi atom as it replaces one of the Sn atoms. The Bi atom generally prefers vertices with additional edges and carries a higher charge density then the Sn atoms because it has a higher unshielded nuclear charge. In order to verify that the theoretical structures are the ground state structures, we compared calculated adiabatic detachment energies and vertical detachment energies with those measured via photoelectron spectroscopy experiments. The ADE represents the energy difference between the ground state of the anionic cluster and that of the neutral ground state geometry. For all of the $BiSn_n^-$ species, the experimental and theoretical values are within error, as can be seen in Table I. The

TABLE I. Theoretical and experimental adiabatic and vertical electron detachment energies, as well as the calculated HOMO-LUMO gaps for the $BiSn_n^-$ clusters. The theoretical VDE2 and VDE3 are excited state transitions (for more information, please refer to the text). Experimental error is ±0.1 eV for ADE and VDE; experimental error is ±0.2 for VDE2 and VDE3. All energies are in electron volts.

	Experimental				Theoretical				
	ADE	VDE	VDE2	VDE3	ADE	VDE	VDE2	VDE3	Gap
1	2.10	2.36	2.64	3.56	2.44	2.51	2.59	2.93	1.87
2	2.20	2.39	2.87	3.26	2.19	2.22	2.95	3.30	1.01
3	2.55	2.81	3.01	3.31,3.63	2.44	2.67	3.27	3.65	1.32
4	2.82	3.18	3.70		2.72	2.92	3.47	3.62	1.92
5	2.52	2.83	3.15	3.4	2.54	2.80	3.36	3.55	1.76
6	2.32	2.72	3.45		2.38	2.59	3.46	3.63	1.26
7	2.65	2.93	3.35	3.35	2.72	2.91	3.51	3.57	0.97
8	2.95	3.26	3.47	3.73	2.97	3.11	3.59	3.70	1.17
9	2.98	3.31	3.55	3.56	2.96	3.06	3.38	3.72	1.40

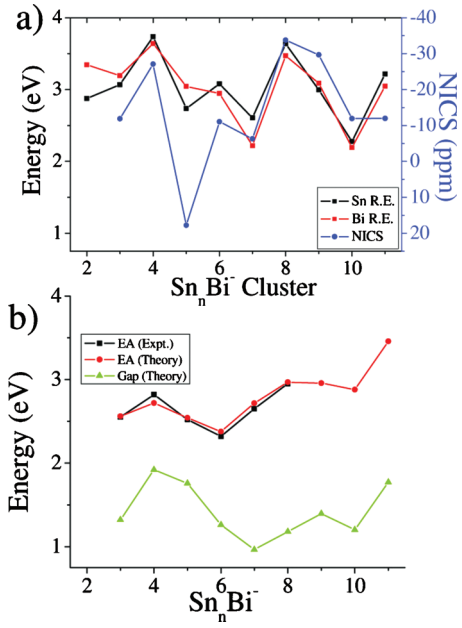

FIG. 4. The Sn and Bi removal energies and NICS values for $BiSn_n^-$ (n =2–11) are given in panel a. The experimental and theoretical adiabatic electron affinities and theoretical HOMO-LUMO gap are given in panel b. Removal energies, electron affinities, and HOMO-LUMO gaps are in electron volts. NICS values are in ppm.

largest discrepancy is for the first cluster species, $BiSn^-$, which has a theoretical ADE of 2.44 eV, while the experimental ADE is 2.10 eV. Additionally, one of the excited state transitions (VDE3) for this species has an experimental value of 3.56 eV, while the theoretical value is 2.93 eV. However, for the other singly doped tin clusters, all of the values agree within acceptable error.

We now turn our attention to the energetics of the $BiSn_n^-$ clusters. A good indicator for a species being stable is the removal energy. The removal energy (RE) is the energy required to remove one Sn or Bi atom from the cluster, defined as

$$\text{Sn}\quad \text{RE} = \text{E(Sn)} + \text{E}(\text{BiSn}_{n-1}^-) - \text{E}(\text{BiSn}_n^-), \tag{1}$$

$$\text{Bi}\quad \text{RE} = \text{E(Bi)} + \text{E}(\text{Sn}_n^-) - \text{E}(\text{BiSn}_n^-). \tag{2}$$

A plot of the removal energies for the clusters can be seen in Fig. 4(a). The largest removal energies correspond to $BiSn_4^-$ and $BiSn_8^-$, which show enhanced abundance in the mass spectrum. $BiSn_7^-$ and $BiSn_{10}^-$ show the smallest removal energies and both show large drops in mass abundance versus adjacent sizes. A plot of the binding energy per atom is found in Fig. S2.[63] A larger gain in energy is also found for $BiSn_4^-$ and $BiSn_8^-$ using this energetic criteria, confirming their enhanced stability. Another way to confirm the magic character is by looking at the energy difference between the LUMO and the HOMO, termed the HOMO-LUMO gap. A large HOMO-LUMO gap is a signature of clusters that show enhanced stability and reduced reactivity.[66] The cluster with the largest gap is $BiSn_4^-$ with a value of 1.92 eV. The second largest gap is that of $BiSn_{11}^-$ (1.78 eV), which is isoelectronic with stannaspherene,[48] and the third largest is $BiSn_5^-$ (1.76 eV), which is expected to have antiaromatic character like Sn_6^{2-}.

To understand the origin of stability of the $BiSn_n^-$ clusters, we next focus on assigning the three-dimensional aromaticity. We performed NICS calculations using the ADF code to quantify the relative aromaticity of the clusters. The NICS was calculated at the center of the cluster and the shifts have been compared with the removal energies in Fig. 4(a). If the cluster is aromatic it will have a negative (diatropic) value and if a cluster is antiaromatic it will have a positive (paratropic) value. We find a significant correlation between the NICS values and the removal energies. $BiSn_4^-$ and $BiSn_8^-$ have the most negative NICS values and they show larger than normal removal energies. Remarkably, $BiSn_5^-$ has significant overall paratropic NICS values and thus is antiaromatic, and $BiSn_7^-$ and $BiSn_6^-$ exhibit the next lowest NICS values and all show reduced stability in both the mass spectra and in the removal energies. It is interesting to note that the NICS values for the doped tin clusters in this study follow a similar trend as for the Sn_n^{2-} clusters previously reported.[50] We also note that size effects may play a role in the NICS value; icosahedral Si_{12}^{2-} is strongly antiaromatic according NICS, while Sn_{12}^{2-} is isoelectronic and yet is nonaromatic, as noted by Zdetsis.[30] Also, there is little correlation observed between the HOMO-LUMO gap and the NICS values.

In order to explore more deeply the evolution of aromatic character throughout these clusters, we have performed a NICS analysis of the individual MO-NICS. The MO-NICS values, the electronic structures, and the isosurfaces of the valence states are given in Fig. 5. First, we note that these clusters show little hybridization between the *s* and *p* states of the atoms, with a gap of 2–3 eV between the molecular orbitals made up of atomic *s* orbitals and those made up of atomic *p* orbitals. In the MO-NICS analysis, the *s* electronic levels all yield a significant diatropic (negative) value. These *s* levels are expected to have little effect on the stability of the cluster. The chemical shifts caused by the *s* electrons increases nearly linearly with the number of atoms, as shown in Table II, so they are not the origin of antiaromaticity or the large variations of NICS with size. The isosurfaces of the *s* levels are similar to the orbitals predicted by free electron gas models such as the jellium model and this delocalization results in induced ring currents which explains the large negative MO-NICS values. However, bonding in these states is much weaker than the *p* states so the importance of the *s* component of NICS is probably not significant with respect to the stability. If one looks at the higher electronic levels, which result from the combination of *p* electrons, there exist much larger variations in the MO-NICS throughout the $BiSn_n^-$ series. For $BiSn_4^-$, the HOMO has a paratropic (positive) value of 17.2, indicating that the HOMO is antiaromatic in character (Fig. 5). However, the HOMO-1, HOMO-2, HOMO-3, etc. all have negative NICS values, bringing the sum of the upper combination of *p* electrons to −0.9 ppm, thus slightly net aromatic. The isosurface of the HOMO, with its highly positive MO-NICS, indicates that this level is a lone pair pointing directly at the center of the cage, with a small amount of bonding in the cage, and a node with neg-

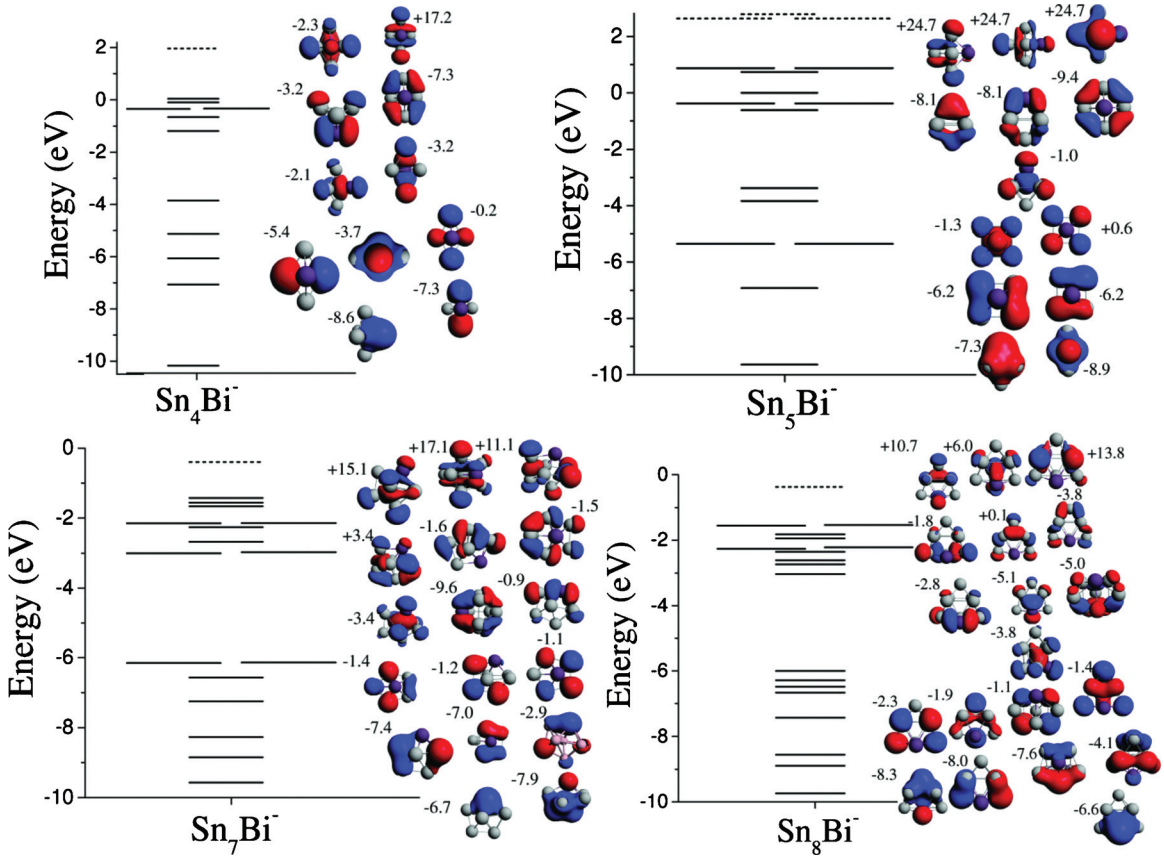

FIG. 5. Electron levels and molecular isosurfaces for $BiSn_4^-$, $BiSn_5^-$, $BiSn_7^-$, and $BiSn_8^-$. The NICS values for each molecular orbital is given in ppm.

ligible charge density in the center of the cage. HOMO-1 through HOMO-3 are all bonding orbitals which allow for ring currents around the cage. In the antiaromatic case of $BiSn_5^-$, the *p* electronic levels show a strikingly large net MO-NICS value of +47.6. Whereas in the Sn_4Bi^- cluster only the HOMO showed antiaromatic character, in Sn_5Bi^- the HOMO, HOMO-1, and HOMO-2 all are antiaromatic, each with values of +24.7 ppm (Fig. 5). All of these levels are lone pair perpendicular to the cage surface and have nodes with minimal charge density at the center of the cage. The overall resulting NICS value is +17.7 ppm, clearly antiaromatic in character.

The positive MO-NICS values of the nonbonding lone pairs in the $BiSn_n^-$ clusters reveal the connection between the NICS values and the stability. As nonbonding orbitals decrease the stability of the cluster, a positive NICS indicates an unusually large amount of charge density in nonbonding orbitals and a relative lack of stability. We note that this phenomenon is quite different from traditional aromaticity in that there is no degeneracy in the electronic spectrum. The reduction in stability is smaller than that in two-dimensional aromaticity and the cluster does not undergo a Jahn–Teller distortion to break the degeneracy. Indeed, $BiSn_5^-$ has a respectable HOMO-LUMO gap and does not require a Jahn–Teller distortion to stabilize the cluster. As noted by King *et al.* and others,[12,30,34] the symmetry of the cluster plays a significant role in the NICS values, as the direction of the lone pair affects the NICS values more strongly than it affects the stability, as $BiSn_7^-$ is the least stable cluster, yet its NICS value is more negative than that of the highly symmetric $BiSn_5^-$. This symmetry effect is caused by the directionality of the lone pair perpendicular to the cage affecting the NICS value more strongly than the actual stability. While antiaromaticity does not result in degeneracies in the electronic state, the reduced stability may still encourage distortions in the geometry. In Fig. 6 we give the ground state of the Sn_6Na^- ion, which distorts to the pentagonal bipyramid structure, despite accepting an electron to form the $[(Sn_6)^{2-}Na^+]$, which would be expected to be the octahedral structure of Fig. 6(b). The isomers of Sn_5Bi^- are shown in Fig. S3 for reference.[63]

TABLE II. NICS values for $BiSn_n^-$ (n=3–8) and the sum of MO-NICS values for the *s* and *p* states (in ppm).

n	$BiSn_n^-$	*s* states	*p* states
3	−11.9	−18.5	7.4
4	−27.1	−25.3	−0.9
5	17.7	−29.3	47.6
6	−11.1	−33.3	21.9
7	−6.3	−35.6	29.8
8	−33.8	−41.3	8.3

V. CONCLUSIONS

We have examined the relative stability of the gas phase Zintl analog $BiSn_n^-$ clusters using both gas phase experiments and theoretical methods. The abundance and detachment energies from the mass spectra and photoelectron spec-

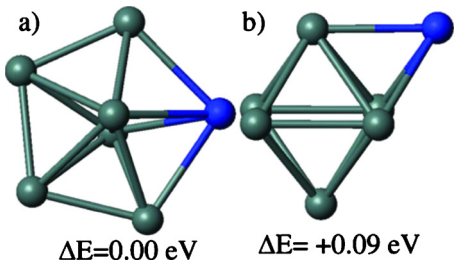

FIG. 6. Geometries of the lowest energy structure (panel a) and isomer (panel b) for the Sn_6Na^- cluster. The gray and blue spheres represent the Sn and Na atoms, respectively. The difference in energy (ΔE) for each of the clusters is given in electron volts.

tra, respectively, along with the calculated removal and electron detachment energies, were compared with their NICS values as a measure of the three-dimensional aromaticity. We find that the NICS values indicate the presence of nonbonding lone pairs perpendicular to the surface of the cluster. This results in reduced stability, although the reduction in stability is small relative to the electronic degeneracies which appear in conventional antiaromaticity. Hence, three-dimensional aromaticity is a useful concept with regards to these inorganic cage clusters, even though it is an imperfect tool for understanding and predicting stability in these clusters.

ACKNOWLEDGMENTS

We gratefully acknowledge financial support from the U.S. Department of the Army through a MURI Grant No. W911NF-06-1-0280. Peneé A. Clayborne and Ujjwal Gupta made equal contributions to the research findings.

[1] J. D. Corbett, Chem. Rev. (Washington, D.C.) **85**, 383 (1985).
[2] S. C. Sevov and J. M. Goicoechea, Organometallics **25**, 5678 (2006).
[3] M. W. Hull and S. C. Sevov, J. Am. Chem. Soc. **131**, 9026 (2009).
[4] R. B. King, I. Silaghi-Dumitrescu, and A. Lupan, Inorg. Chem. **45**, 4974 (2006).
[5] T. K. Bera, J. I. Jang, J. B. Ketterson, and M. G. Kanatzidis, J. Am. Chem. Soc. **131**, 75 (2009).
[6] S. A. Claridge, A. W. Castleman, Jr., S. N. Khanna, C. B. Murray, A. Sen, and P. S. Weiss, ACS Nano **3**, 244 (2009).
[7] P. D. Jadzinsky, G. Calero, C. J. Ackerson, D. A. Bushnell, and R. D. Kornberg, Science **318**, 430 (2007).
[8] A. E. Riley, S. D. Korlann, E. K. Richman, and S. H. Tolbert, Angew. Chem., Int. Ed. **45**, 235 (2006).
[9] S. D. Korlann, A. E. Riley, B. S. Mun, and S. H. Tolbert, J. Phys. Chem. C **113**, 7697 (2009).
[10] M. Qian, A. C. Reber, A. Ugrinov, N. K. Chaki, S. Mandal, H. Saavedra, S. N. Khanna, A. Sen, and P. S. Weiss, ACS Nano **4**, 235 (2010).
[11] R. B. King and I. Silaghi-Dumitrescu, Dalton Trans., 6083 (2008).
[12] C. Corminboeuf, R. B. King, and P. R. Schleyer, ChemPhysChem **8**, 391 (2007).
[13] R. B. King, I. Silaghi-Dumitrescu, and A. Kun, J. Chem. Soc. Dalton Trans., 3999 (2002).
[14] R. B. King, I. Silaghi-Dumitrescu, and A. Kun, Inorg. Chem. **40**, 2450 (2001).
[15] P. J. Roach, W. H. Woodward, A. C. Reber, S. N. Khanna, and A. W. Castleman, Jr., Phys. Rev. B **81**, 195404 (2010).
[16] P. J. Roach, W. H. Woodward, A. W. Castleman, Jr., A. C. Reber, and S. N. Khanna, Science **323**, 492 (2009).
[17] A. C. Reber, S. N. Khanna, P. J. Roach, W. H. Woodward, and A. W. Castleman, Jr., J. Phys. Chem. A **114**, 6071 (2010).
[18] A. W. Castleman, Jr., S. N. Khanna, A. Sen, A. C. Reber, M. Qian, K. M. Davis, S. J. Peppernick, A. Ugrinov, and M. D. Merritt, Nano Lett. **7**, 2734 (2007).
[19] U. Gupta, A. C. Reber, P. A. Clayborne, J. J. Melko, S. N. Khanna, and A. W. Castleman, Jr., Inorg. Chem. **47**, 10953 (2008).
[20] R. W. Farley and A. W. Castleman, Jr., J. Chem. Phys. **92**, 1790 (1990).
[21] R. W. Farley, P. Ziemann, and A. W. Castleman, Jr., Z. Phys. D: At., Mol. Clusters **14**, 353 (1989).
[22] R. W. Farley and A. W. Castleman, Jr., J. Am. Chem. Soc. **111**, 2734 (1989).
[23] K. LaiHing, P. Y. Cheng, W. L. Wilson, and M. A. Duncan, J. Chem. Phys. **88**, 2831 (1988).
[24] R. G. Wheeler, K. LaiHing, W. L. Wilson, J. D. Allen, R. B. King, and M. A. Duncan, J. Am. Chem. Soc. **108**, 8101 (1986).
[25] U. Gupta, J. U. Reveles, J. J. Melko, S. N. Khanna, and A. W. Castleman, Jr., Chem. Phys. Lett. **467**, 223 (2009).
[26] U. Gupta, J. U. Reveles, J. J. Melko, S. N. Khanna, and A. W. Castleman, Jr., Chem. Phys. Lett. **480**, 189 (2009).
[27] M. A. Sobhy, J. U. Reveles, U. Gupta, S. N. Khanna, and A. W. Castleman, Jr., J. Chem. Phys. **130**, 054304 (2009).
[28] Z. Sun, Q. H. Zhu, Z. Gao, and Z. C. Tang, Rapid Commun. Mass Spectrom. **23**, 2663 (2009).
[29] A. D. Zdetsis, J. Phys. Chem. A **113**, 12079 (2009).
[30] A. D. Zdetsis, J. Chem. Phys. **131**, 224310 (2009).
[31] K. Wade, J. Chem. Soc., Chem. Commun. **15**, 792 (1971).
[32] D. M. P. Mingos, Nat. Phys. Sci. **236**, 99 (1972).
[33] A. Hirsch, Z. Chen, and J. Haijun, Angew. Chem. **113**, 2916 (2001).
[34] R. B. King, T. Heine, C. Corminboeuf, and P. R. von Schleyer, J. Am. Chem. Soc. **126**, 430 (2004).
[35] Z. Chen and R. B. King, Chem. Rev. (Washington, D.C.) **105**, 3613 (2005).
[36] A. Hirsch, Z. Chen, and H. Jiao, Angew. Chem., Int. Ed. **40**, 2834 (2001).
[37] P. Garrat, *Aromaticity* (Wiley, New York, 1986).
[38] E. Hückel, Z. Phys. **70**, 204 (1931).
[39] X. Li, A. Kuznetsov, H. Zhang, A. Boldyrev, and L. S. Wang, Science **291**, 859 (2001).
[40] J. J. Melko, P. A. Clayborne, C. E. Jones, Jr., J. U. Reveles, U. Gupta, S. N. Khanna, and A. W. Castleman, Jr., J. Phys. Chem. A **114**, 2045 (2010).
[41] C. E. Jones, Jr., P. A. Clayborne, J. U. Reveles, U. Gupta, J. J. Melko, A. W. Castleman, Jr., and S. N. Khanna, J. Phys. Chem. A **112**, 13316 (2008).
[42] A. Ugrinov, A. Sen, A. C. Reber, M. Qian, and S. N. Khanna, J. Am. Chem. Soc. **130**, 782 (2008).
[43] A. Hirsch, Z. Chen, and H. Jiao, Angew. Chem., Int. Ed. **39**, 3915 (2000).
[44] P. R. Schleyer, C. Maeker, A. Dransfeld, H. Jiao, and N. J. R. van Eikema Hommes, J. Am. Chem. Soc. **118**, 6317 (1996).
[45] Z. F. Chen, C. S. Wannere, C. Corminboeuf, R. Puchta, and P. R. Schleyer, Chem. Rev. (Washington, D.C.) **105**, 3842 (2005).
[46] A. E. Kuznetsov, K. A. Birch, A. I. Boldyrev, X. Li, H.-J. Zhai, and L. S. Wang, Science **300**, 622 (2003).
[47] Z. Chen, C. Corminboeuf, T. Heine, J. Bohmann, and P. V. Ragué Schleyer, J. Am. Chem. Soc. **125**, 13930 (2003).
[48] L. F. Cui, X. Huang, L. M. Wang, D. Y. Zubarev, A. I. Boldyrev, J. Li, and L. S. Wang, J. Am. Chem. Soc. **128**, 8390 (2006).
[49] L. F. Cui, X. Huang, L. M. Wang, J. Li, and L. S. Wang, Angew. Chem., Int. Ed. **46**, 742 (2007).
[50] D. Y. Zubarev, A. N. Alexandrova, A. I. Boldyrev, L. F. Cui, X. Li, and L. S. Wang, J. Chem. Phys. **124**, 124305 (2006).
[51] Z. Chen, S. Neukermans, X. Wang, E. Janssens, Z. Zhou, R. Silverans, R. B. King, P. R. Schleyer, and P. Lievens, J. Am. Chem. Soc. **128**, 12829 (2006).
[52] B. Schiemenz and G. Huttner, Angew. Chem., Int. Ed. Engl. **32**, 297 (1993).
[53] K. L. Knappenberger, C. E. Jones, M. A. Sobhy, and A. W. Castleman, Jr., Rev. Sci. Instrum. **77**, 123901 (2006).
[54] W. C. Wiley and I. H. McLaren, Rev. Sci. Instrum. **26**, 1150 (1955).
[55] P. Kruit and F. H. Read, J. Phys. E **16**, 313 (1983).
[56] V. Dribinski, A. Ossadtchi, V. A. Mandelshtam, and H. Reisler, Rev. Sci. Instrum. **73**, 2634 (2002).
[57] G. te Velde, F. M. Bickelhaupt, E. J. Baerends, C. Fonseca Guerra, S. J. A. van Gisbergen, J. G. Snijders, and T. Ziegler, J. Comput. Chem. **22**, 931 (2001).
[58] A. D. Becke, Phys. Rev. A **38**, 3098 (1988).
[59] J. P. Perdew, Phys. Rev. B **33**, 8822 (1986).

[60] J. P. Perdew, K. Burke, and M. Enzerhof, Phys. Rev. Lett. **77**, 3865 (1996).
[61] C. Fonseca Guerra, J. G. Snijders, G. te Velde, and E. J. Baerends, Theor. Chem. Acc. **99**, 391 (1998).
[62] T. Heine, P. V. Rague Schleyer, C. Corminboeuf, G. Seifert, R. Reviakine, and J. Weber, J. Phys. Chem. A **107**, 6470 (2003).
[63] See supplementary material at http://dx.doi.org/10.1063/1.3488103 for a comparison of the molecular orbitals for the Sn_5^{2-} and $BiSn_4^-$ clusters, Beta parameters of $BiSn_n^-$ (n=1–6), a plot of binding energy per atom, and Cartesian coordinates of the anion and neutral bismuth doped tin clusters.
[64] A. C. Reber, A. Ugrinov, A. Sen, M. Qian, and S. N. Khanna, Chem. Phys. Lett. **473**, 305 (2009).
[65] S. Sun, H. Liu, and Z. Tang, J. Phys. Chem. A **110**, 5004 (2006).
[66] A. C. Reber, S. N. Khanna, P. J. Roach, W. H. Woodward, and A. W. Castleman, Jr., J. Am. Chem. Soc. **129**, 16098 (2007).